Use of rheometry and H−1 NMR spectroscopy for understanding the mechanisms behind the generation of coking pressure

ARTICLE *in* ENERGY & FUELS · SEPTEMBER 2004

Impact Factor: 2.79 · DOI: 10.1021/ef0340581

4 AUTHORS:

K. M. Steel
University of Queensland
51 PUBLICATIONS **472** CITATIONS
SEE PROFILE

M. Castro Diaz
University of Nottingham
30 PUBLICATIONS **188** CITATIONS
SEE PROFILE

John Patrick
University of Nottingham
104 PUBLICATIONS **1,460** CITATIONS
SEE PROFILE

Colin E. Snape
University of Nottingham
435 PUBLICATIONS **7,248** CITATIONS
SEE PROFILE

Use of Rheometry and ^{1}H NMR Spectroscopy for Understanding the Mechanisms behind the Generation of Coking Pressure

Karen M. Steel,* Miguel Castro Diaz, John W. Patrick, and Colin E. Snape

Nottingham Fuel and Energy Centre, School of Chemical, Environmental and Mining Engineering, Nottingham University, Nottingham, NG7 2RD, United Kingdom

Received September 19, 2003. Revised Manuscript Received May 20, 2004

The fluid phase which forms during carbonization of a range of coals was studied using rheometry and ^{1}H NMR spectroscopy to study the mechanisms behind the generation of excessive wall pressures during coking. It is proposed that high coking pressures are generated for low volatile matter coals when the temperature of maximum fluidity (T_{mf}) is >465 °C, the minimum complex viscosity (η^*) is $>10^5$ Pa s, the percentage of mobile ^{1}H (fluid phase) is <40%, and the ^{1}H mobility in the fluid phase is <65 μs. It is suggested for these coals that the particles fuse to form a rigid network containing pockets of fluid material which have a low fluidity and do not link up. This arrangement could present an impermeable barrier for gas flow and force the gas to the coal side where it builds up in a diminishing region to a critical level, causing pressure on the walls. The magnitude of the pressure generated may be proportional to T_{mf} and η^* and inversely proportional to the percentage and mobility of mobile ^{1}H. It was also found that a high volatile coal which formed a highly fluid phase over a broad temperature range gave rise to a significant coking pressure. In this case, it is proposed that the sheer expansion of the coal charge as it converts to gas and liquid phases is the reason for pressure on the oven walls. These proposals agree with current thinking on the generation of coking pressure. This work is based on the testing of only nine samples and further work is planned to gain a greater fundamental understanding of fluidity development from which models for predicting coking pressure and coke quality for coal blends may be developed.

Introduction

In the process of forming metallurgical coke, coal is heated in the absence of oxygen to cause both phase changes and chemical reactions to take place that lead to the release of volatile compounds and the softening of the coal to form a fluid phase. The temperature at which softening starts depends on coal rank, particle size, and heating rate, and is usually around 400 °C. Upon further heating, the viscosity of the fluid phase decreases to a minimum and the rate of volatile release reaches a maximum. As temperatures increase still further, the viscosity increases as the softened mass resolidifies, leading to the final coke product.[1] The coking of certain coals can cause excessive pressure to be exerted on the oven walls which is damaging. The reasons why certain coals give rise to high coking pressures are still largely unknown, and there are no simple and precise tests for predicting coking pressure for a given coal.

Graphs of coking pressure plotted against time generally show two peaks which vary significantly in size between different coals.[2] The first peak occurs early in the process and is usually broad, while the second peak is sharper and occurs toward the end of the process. These peaks are thought to be due to two different events occurring at different stages of the coking process. In the first stage, the temperature at the coal charge center is <350 °C and there are two plastic layers surrounding unfused coal. It is thought that pressure on the walls during this phase may be due to swelling of the plastic zone, and connected to the equilibrium between swelling of the plastic zone and contraction of the semicoke. In the second stage, the temperature at the coal charge center is >350 °C. In this stage, the two plastic layers meet and there is a sharp increase in pressure on the walls. It is thought that the pressure may be caused by gases becoming trapped in the diminishing coal region, accumulating, and causing pressure to be exerted on the oven walls. The equilibrium between swelling and contraction will also play a part in this event. A relationship between the extent to which coal contracts during carbonization and wall pressure has been identified,[3] which shows that the lower the degree of contraction, the higher the wall pressure generated. It was also found that contraction, and therefore wall pressure, is related to the vapor phase composition. When lower alkylated aromatics dominate the vapor phase, the degree of contraction is low. Furthermore, when the temperature of maximum fluidity (T_{mf}) and resolidification (T_r) are greater than

* Corresponding author. Tel: +44-115-9514078. Fax: +44-115-9514115. E-mail: karen.steel@nottingham.ac.uk.

(1) Elliot, M. A. *Chemistry of coal utilization. Second supplementary volume*; John Wiley and Sons: New York, 1981; pp 338−358.

(2) Loison, R.; Foch, P.; Boyer, A. *Coke - Quality and Production*; Butterworths: Markham, ON, Canada, 1989; p 369.

(3) Marzec, A.; Czajkowska, S.; Alvarez, R.; Pis, J. J.; Diez, M. A.; Schulten, H. *Energy Fuels* **1997**, *11*, 982−986.

10.1021/ef034058l CCC: $27.50
Published on Web 06/30/2004

approximately 455 °C and 485 °C, respectively, the extent to which the coal contracts decreases with increasing T_{mf} and T_r.[4] It has also been found that for high coking pressure coals, the rate of volatile release tends to reach a maximum at a temperature higher than the T_{mf}.[5]

With regard to the second event, the reason or likelihood of gases accumulating in the center of the coal charge is thought to be connected to the viscosity of the fluid phase. For the last 60 years, fluidity measurements have been made using a Gieseler plastometer[6] which has provided valuable empirical measurements of fluidity. However, these measurements have not provided a useful model with which to predict coking pressure. Rheometry and ^{1}H nuclear magnetic resonance (NMR) spectroscopy techniques are brought together in this paper to study the fluid phase and elucidate possible mechanisms for coking pressure from which a model might be developed for predicting coking pressure for a given coal.

A high-torque rheometer has been used to measure the linear viscoelastic properties of the coal samples. The measurement involves placing a sample between two parallel plates. One plate is connected to a motor which moves the surface sinusoidally. The variable parameters in the movement are the frequency (ω) (number of oscillations per second) and the strain (γ) (angular displacement from the zero position). The samples stress response (τ) to this oscillatory deformation is measured by a transducer connected to the other plate.

If the sample is an ideal elastic material, the strain and stress curves over time are the same, and if the sample is an ideal viscous material, the strain and stress curves over time are out of phase by 90°. By measuring the phase shift or phase angle (δ), information about the viscoelastic behavior of the sample can be obtained, i.e., for viscoelastic materials $0 < \delta < 90°$.

The storage modulus (G') is proportional to the elastic energy which is stored and recovered, and the loss modulus (G'') is proportional to the energy dissipated in flow. G' and G'' are given by eqs 1 and 2.[7]

$$G' = \tau_0/\gamma_0 \cos \delta \quad (1)$$

$$G'' = \tau_0/\gamma_0 \sin \delta \quad (2)$$

where τ_0 is the maximum stress response measured in the sinusoidal motion and γ_0 is the maximum applied strain in the sinusoidal motion.

The complex viscosity (η^*) is given by eq 3.

$$|\eta^*| = \{(G'^2 + G''^2)^{(1/2)}\}/\omega \quad (3)$$

Another important parameter is tan δ, which is the ratio of G'' to G', given by eq 4.

$$\tan \delta = G''/G' \quad (4)$$

When tan $\delta > 1$, viscous properties dominate, and when tan $\delta < 1$, elastic properties dominate.

It is important that all tests are conducted in the "linear viscoelastic region". This means that the response of the sample (stress) is directly proportional to the value of the initiating signal (strain). The differential equations which describe the flow behavior are then linear, which makes the mathematical expressions for describing the flow far simpler than those for nonlinear viscoelastic behavior. This, in turn, makes it easier to understand the microstructural changes taking place in the sample as it flows. To test whether the rheometer is operating in the linear viscoelastic region (LVR), a strain sweep test is performed where the strain is varied and G' and G'' are measured. G' and G'' are constant with strain rate in the LVR. If measurements are not in the LVR, the results are dependent on experimental details and are more difficult to relate to the unique properties of the material.

Nomura et al.[8] showed that small amplitude oscillatory shear rheometry could be used to measure the viscoelastic properties of coal. Studies on a range of coals showed that as softening began at around 400 °C, η^* decreased to a minimum value before increasing at higher temperatures. Complex viscosities of the coals studied were found to lie in the range of 1×10^4 to 6×10^5 Pa s, using a γ and ω of 0.1% and 6.28 rad/s, respectively. Variation in ω showed that the fluid phase was shear thinning. Therefore, it was suggested that the Gieseler plastometer may underestimate the minimum viscosity due to structural changes incurred by the higher shear rates. Further work by Yoshida et al.[9] on 10 coals compared results obtained from the rheometer and the Gieseler plastometer and found that the temperatures at which changes occur were in fairly good agreement.

The second technique used to measure fluidity during carbonization is high temperature ^{1}H nuclear magnetic resonance (NMR) spectroscopy. This technique determines the fluidity evolving in a sample through the analysis of spectra acquired at different temperatures. The spectra are usually deconvoluted into two components, namely, a Lorentzian distribution function that originates from the protons associated with the mobile phase in the sample, and a Gaussian distribution function that originates from the protons associated with the rigid phase. The fraction of fluid phase in the sample can be calculated by

$$\% \text{ fluid} = A_L/(A_L + A_G) \quad (5)$$

where A_L and A_G represent the areas of the Lorentzian and Gaussian functions, respectively. Further, the spin−spin relaxation time (T_2) is inversely proportional to the peak width at half-height ($\Delta H_{(1/2)}$) as indicated by eq 6 and gives information about the mobility of the phase.

$$T_2 = 1/(\pi \Delta H_{(1/2)}) \quad (6)$$

Although this straightforward relationship is fulfilled only for Lorentzian distribution functions, it is generally

(4) Alvarez, R.; Pis, J. J.; Diez, M. A.; Marzec, A.; Czajkowska, S. *Energy Fuels* **1997**, *11*, 978−981.
(5) Barriocanal, C.; Hays, D.; Patrick, J. W.; Walker, A. *Fuel* **1998**, *77*, 729−733.
(6) Standard Test Method for Plastic Properties of Coal by the Constant-Torque Gieseler Plastometer. *American Standard for Testing Materials (ASTM)*: 1997; D 2639-97.
(7) Steffe, J. F. *Rheological Methods in Food Process Engineering*; Freeman Press: East Lansing, MI, 1996; p 315.
(8) Nomura, S.; Kato, K.; Komaki, I.; Fujioka, Y.; Saito, K.; Yamaoka, I. *Fuel* **1999**, *78*, 1583−1589.
(9) Yoshida, T.; Iino, M.; Takanohashi, T.; Katoh, K. *Fuel* **2000**, *79*, 399−404.

Table 1. Properties of Coal Samples. T_s, T_{mf}, and T_r Are Temperatures for Softening, Maximum Fluidity, and Re-solidification, Respectively

			Gieseler				
coal	volatile matter daf (wt %)	swelling index	T_s (°C)	T_{mf} (°C)	T_r (°C)	maximum fluidity (ddpm)	wall pressure 250 kg oven (kPa)
C1	32.8	6.75	387	448	489	29783	3.0
C2	19.3	8.00	439	473	500	37	15.9
C3	17.9	7.75	440	479	507	37	48.4
C4	32.1	5.50	381	443	486	26810	2.0
C5	25.3	6.75	400	452	487	1726	2.4
C6	26.1	8.00	396	454	493	2954	3.7[a]
B1	19.5		418	457	487	94	4.1[b]
B2	18		436	466	487	16	5.8[b]
B3	17.1		442	460	486	6	12.9[b]
C5	25.3	6.75	400	452	487	1726	1.2[b]
C6	26.1	8.00	396	454	493	2954	7.1[b]

[a] Coal C6 is known to generate wall pressures higher than 3.7 kPa and to generate reduced pressures when blended with lower fluidity coals that do not generate wall pressures. [b] 25 kg oven, internal gas pressure (not wall pressure).

used to determine the mobility of both fluid and rigid phases. As $\Delta H_{(1/2)}$ decreases, T_2 increases, indicating that ^{1}H mobility is increasing.[10]

This technique has been used to determine the concentration and mobility of the fluid and rigid phases in coals,[11,12] to characterize the extent of fusion or interaction between components of a blend during carbonization[13,14] and to elucidate the effect of macerals on fluidity development.[15] In a more detailed work, Sakurovs[16] found that Australian coking coal blends undergo significant positive and negative interactions, which increase with increasing difference in rank and fluidity between the coals. Moreover, these interactions were directly related to the fluid material evolving from inertinite and vitrinite. More recently, Hayashi et al.[17,18] combined ^{1}H NMR spectroscopy with needle penetrometry to study the morphology of coal samples during pyrolysis. The softened mass was assumed to behave as a suspension of solid particles in a liquid medium, with the fraction of mobile hydrogen (ϕ_{mh}) being a measure of the liquid fraction. The relationship between log viscosity and ϕ_{mh} was found to be linear in the region of $0.1 < \phi_{mh} < 0.5$. Coal samples giving higher values of ϕ_{mh} were not studied.

Experimental Section

A range of coal samples with varying coking behaviors were tested. Table 1 shows properties of the samples, including Gieseler and coking pressure data. B1, B2, and B3 are blends with compositions given in Table 2. The samples contain an increasing concentration of C7 coal from B1 to B3. Table 3 shows petrographic analysis for coals C1−C4.

Table 2. Composition of B1, B2, and B3 Coal Blends

Coal blend	C7 (%)	Amonate (%)	Marfork (%)	Coke dust (%)	Ash (%)
B1	40	40	10	10	7.1
B2	50	40	0	10	6.8
B3	70	20	0	10	5.8

Table 3. Petrographic Analysis of Coals C1−C4

	Composition (%)				Mean reflectance
	Vitrinite	Exinite	Semi-fusinite	Inertinite	
C1	71.9	5.5	16.9	5.7	0.95
C2	91.6	5.6	16.4	6.1	0.92
C3	82.7	0.1	12.9	4.3	1.52
C4	71.9	0.0	5.8	2.6	1.40

Coking tests for the determination of wall pressure were carried out in a 250 kg moveable wall oven at the Instituto Nacional del Carbón (INCAR), CSIC, in Spain.[19] Gieseler plastometer tests for coal samples C1−C6 were carried out at INCAR. Coking tests for the determination of internal gas pressure were carried out in a 25 kg oven at the Centre de Pyrolyse de Marienau (CPM) in France.[19] Gieseler tests for blends B1−B3 were carried out at CPM.

Rheological measurements were performed using a Rheometrics RDA-III high-torque controlled strain rheometer. Coal samples (1.5 g, <53 μm) were pressed under 5 tonnes of pressure in a 25 mm die to form disks with a thickness of approximately 2.6 mm. The test involved placing the disk of coal between two 25 mm parallel plates, which had serrated surfaces to reduce "slippage". The sample was heated quickly to 330 °C and then heated to 600 °C at a rate of 3 °C/min. The furnace surrounding the sample was purged with a constant flow of N_2 to transfer heat to the sample and remove volatiles. The sample temperature was monitored using a thermocouple in direct contact with the bottom plate. Initially, strain sweep tests were performed on C1 coal to ensure that measurements were in the LVR. The strain sweeps, which took 1.5 min, were performed at 375 °C, 400 °C, 430 °C, and 445 °C. At 375 °C and 400 °C, the LVR was in the strain region $\gamma = 0.003\%-0.1\%$; at 430 °C and 445 °C, the LVR was in the full strain region measured $\gamma = 0.003\%-0.5\%$. Following this, tests were performed with a strain of amplitude 0.1% and a frequency of 1 Hz (6.28 rad/s). This was applied to the sample from the bottom plate throughout the heating period. The stress response on the top plate was measured to obtain G', G'', and η^* as a function of temperature. Throughout the test, a constant normal force of 200 g was applied to the sample from the top plate to reduce slippage. Therefore, the thickness of the sample was allowed to change. The thickness could be measured throughout the test and gives an indication of how much the sample is expanding/contracting.

A Doty 200 MHz ^{1}H NMR probe was used with a Bruker MSL300 instrument for the NMR fluidity development studies. The assembly was placed horizontally in the stator. A flow of 16 dm^3/min of dry nitrogen was used to transfer heat to the samples and to remove the volatiles that escape from the container. Below the sample region, a flow of 65−70 dm^3/min of dry air prevented the temperature rising above 50 °C to protect the electrical components. In addition, air was blown at 20 dm^3/min into the region between the top bell Dewar enclosing the sample region and the outer side of the probe to prevent the temperature from exceeding 110 °C. The sample temperature was monitored using a thermocouple in direct contact with the sample container. The solid echo pulse sequence (90°−τ−90°) was used to determine the variation in peak width as a function of temperature. The pulse length was increased from 3.5 μs at room temperature to 4.85 μs at the

(10) Sakurovs, R.; Lynch, L. J.; Barton, W. A. *Magnetic Resonance of Carbonaceous Solids*; Botto, R. E., Sanada, Y., Eds.; Advances in Chemistry Series 229; American Chemical Society: Washington, DC, 1993; pp 229−251.
(11) Maroto-Valer, M. M.; Andrésen, J. M.; Snape, C. E. *Fuel* **1998**, *77*, 921−926.
(12) Snape, C. E.; Martin, S. C. *Prepr. Symp. Am. Chem. Soc., Div. Fuel Chem.* **2000**, *45* (2), 205−210.
(13) Sakurovs, R.; Lynch, L. J. *Fuel* **1993**, *72*, 743−749.
(14) Sakurovs, R.; Lynch, L. J.; Maher, T. P. *Fuel Process. Technol.* **1994**, *37*, 255−269.
(15) Maroto-Valer, M. M.; Taulbee, D. N.; Andrésen, J. M.; Hower, J. C.; Snape, C. E. *Energy Fuels* **1998**, *12*, 1040−1046.
(16) Sakurovs, R. *Fuel* **2003**, *82*, 439−450.
(17) Hayashi, J.; Morita, M.; Moriyama, R.; Chiba, T. *Fuel* **2003**, *82*, 1735−1741.
(18) Hayashi, J.; Morita, M.; Chiba, T. *Fuel* **2003**, *82*, 1743−1750.
(19) Reports for the European Coal and Steel Community (now Research Fund for Coal and Steel). Contracts 7220-PR/069 2003 and 7220-PR/119 (current).

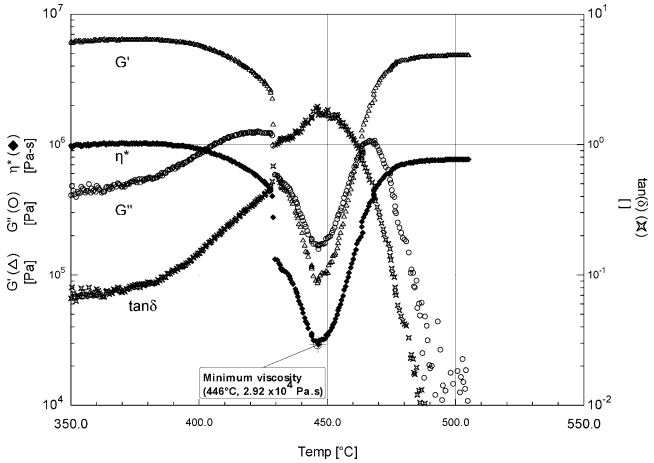

Figure 1. Viscoelastic properties of C1 coal as a function of temperature. ($\gamma = 0.1\%$, $\omega = 6.28$ rad/s)

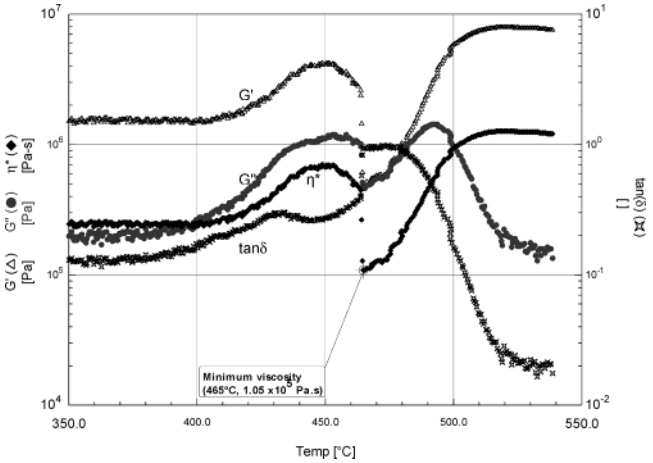

Figure 2. Viscoelastic properties of C2 coal as a function of temperature. ($\gamma = 0.1\%$, $\omega = 6.28$ rad/s)

final temperature. Approximately 140−150 mg of sample (<53 μm) was packed lightly into a boron nitride container, and 200 scans were accumulated using a recycle delay of 0.3 s. The samples were heated from room temperature to 320 °C at approximately 60 °C/min and then at a rate of approximately 3 °C/min to the final temperature. The spectra obtained between approximately 280 °C and 480 °C were deconvoluted into Gaussian and Lorentzian components, and the proportions of mobile and rigid phases together with their mobilities were determined. Measurements were also made using particles in the size range 53-212 μm, as it has been found that smaller particles have reduced fluidity.[20]

Results

Rheometry. Figure 1 shows the viscoelastic properties of C1 coal as it is heated from 350 °C to 500 °C at a rate of 3 °C/min. At temperatures less than 400 °C, G' remains constant, indicating that there is little change taking place in the sample. $G' > G''$ and tan $\delta < 1$, indicating that elastic properties dominate. As the temperature exceeds 400 °C, G' gradually decreases, G'' increases, and tan δ increases, indicating that the sample is softening and becoming less elastic. At 428 °C, there is a dramatic change and the sample becomes considerably less elastic. G' drops, and tan δ exceeds one, indicating that viscous forces dominate over elastic forces. The material behaves more like a fluid and η^* reaches a minimum value of 2.92×10^4 Pa s at 446 °C. As the temperature increases above 446 °C, elasticity increases and the sample begins to resolidify. Tan δ drops back below one at 462 °C, and resolidification is almost complete at 480 °C.

Figure 2 shows the viscoelastic properties of C2 coal. Like C1 coal, there is little change in C2 at temperatures up to 400 °C. Above 400 °C, η^* begins to increase. This is due to G' increasing. While G' increases, G'' increases at a greater rate so tan δ increases, indicating that the sample is becoming less elastic. It should be noted here that the disk of coal is not a solid piece of coal but rather a disk of compressed coal particles of <53 μm. Therefore, it is possible that, at the lower temperatures, the particles slip past each other under the strain and this would have an effect on the properties measured. In particular, slipping gives rise to a reduced G'. As the temperature increases above 450 °C, softening becomes far more pronounced and η^* begins to decrease, decreasing markedly at 464 °C to a minimum of 1.05×10^5 Pa s at 465 °C. Above 465 °C, the sample begins to resolidify with resolidification essentially complete by 510 °C. Compared to C1 coal, C2 does not become as fluid and reaches its minimum η^* of approximately 10^5 Pa s at a higher temperature. In addition, tan δ does not exceed one.

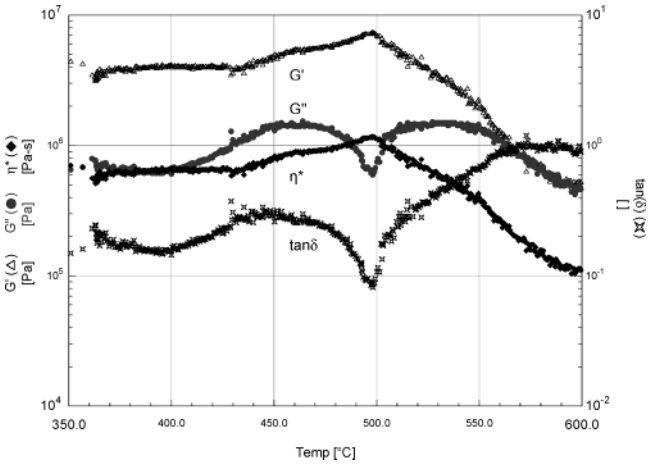

Figure 3. Viscoelastic properties of C3 coal as a function of temperature. ($\gamma = 0.1\%$, $\omega = 6.28$ rad/s)

Figure 3 shows the viscoelastic properties of C3 coal. No distinct fluid phase was detected for C3 coal, although G'' does increase to a maximum of 1.5×10^6 Pa at 464 °C. Interestingly, G' and η^* begin to decrease at 500 °C, with η^* decreasing to 1.1×10^5 Pa s at 600 °C. The reason for this behavior is not known. Reducing both the strain and frequency to 0.02% and 0.5 rad/s, respectively, had virtually no effect on the behavior observed.

Figure 4 shows the complex viscosity of three coal blends, which have an increasing concentration of C7 coal from B1 to B3 (compositions shown in Table 2). All samples began to soften slightly at 440 °C and more considerably at 460 °C, 465 °C, and 480 °C for B1, B2, and B3, respectively. Complex viscosities decrease to similar minimum values of approximately 2×10^5 Pa s. However, this occurs at different temperatures of 467 °C, 471 °C, and 485 °C for B1, B2, and B3, respectively. Tan δ reached one for B1 and B2, but not for B3. The temperature range at which the samples are fluid

(20) Maroto-Valer, M. M.; Andrésen, J. M.; Snape, C. E. *Energy Fuels* **1997**, *11*, 236−244.

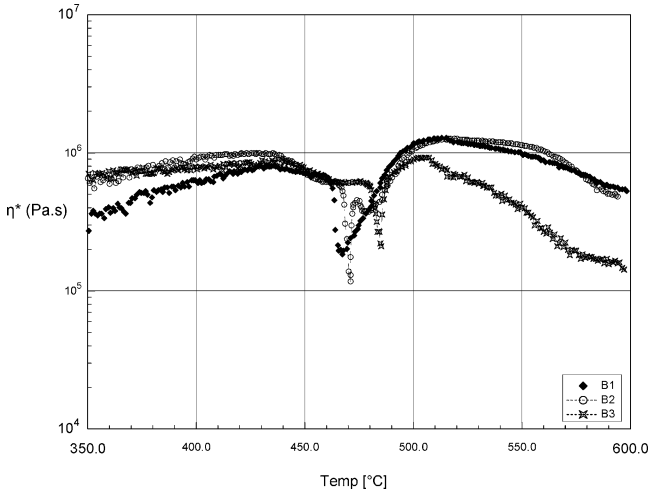

Figure 4. Complex viscosity of B1, B2, and B3 coal blends as a function of temperature. ($\gamma = 0.1\%$, $\omega = 6.28$ rad/s)

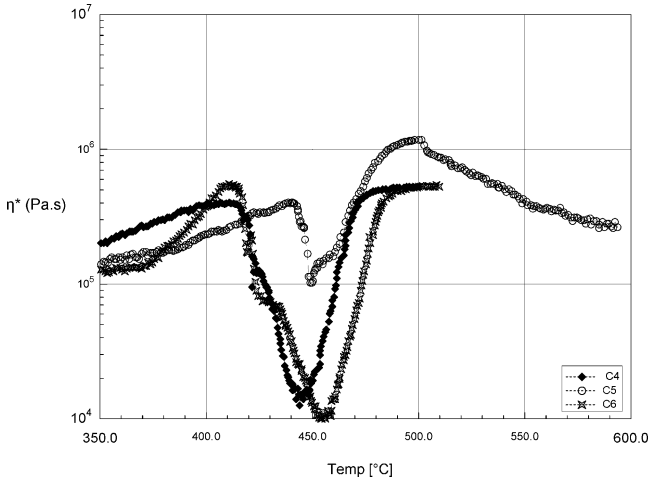

Figure 5. Complex viscosity of C4, C5, and C6 coals as a function of temperature. ($\gamma = 0.1\%$, $\omega = 6.28$ rad/s)

decreases substantially from B1 to B3. The complex viscosity for B3 decreases above 500 °C in a way similar to that observed for C3.

Figure 5 shows the complex viscosity of C4, C5, and C6 coals. The complex viscosity curve for C4 is very similar to C1, shown in Figure 1, with a minimum η^* of 1.26×10^4 Pa s. C5 shows a behavior similar to that of C2 and B1, with η^* decreasing to only 1.03×10^5 Pa s, yet this minimum η^* occurs at a lower temperature of 450 °C. C6 was found to be the most fluid coal measured, with η^* decreasing to 1×10^4 Pa s at 455 °C and the fluid region persisting over a wide temperature range.

^{1}H NMR Spectroscopy. Figure 6 shows the effect of percentage fluid phase and ^{1}H mobility in the spectra for C1, C5, and B3 coals at the temperature of maximum fluidity (T_{mf}) which is the temperature of maximum percentage of fluid phase. The percentage decreases from C1 coal to C5 coal and to B3 coal, and the ^{1}H mobility also decreases in that order.

Figure 7 shows the percentage fluid phase as a function of carbonization temperature for all coals studied. T_{mf} increases in the approximate order of C4 < C1 < C5 < B2 ~ C6 < B1 < C2 < C3 < B3, and percentage fluid phase increases in roughly the reverse order of C3 ~ C2 < B3 < C5 ~ B2 ~ B1 < C6 < C1 <

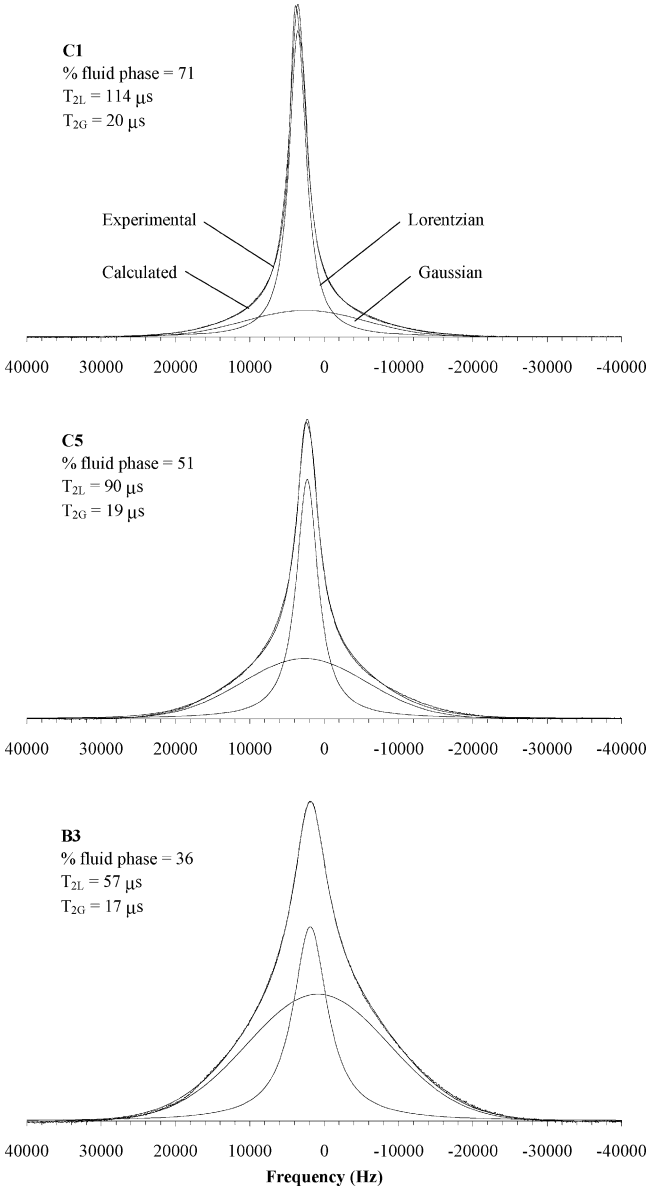

Figure 6. Deconvoluted ^{1}H NMR spectra of samples C1, C5, and B3 at the temperature of maximum percentage of fluid phase (particle size 53−212 μm).

C4. Figure 8 shows the ^{1}H mobility of the fluid phase, expressed as the T_2 of the Lorentzian distribution (T_{2L}), as a function of temperature. T_{2L} increases in the approximate order of B1 ~ B2 ~ B3 < C3 < C2 < C4 < C5 < C6 < C1. Generally, the mobility of the fluid phase increases with increasing percentage of fluid phase for coals with very different fluidities, but this trend does not occur when the fluidity of the coals is similar. In addition, T_{mf} is not necessarily the temperature at which the mobility is at a maximum. Table 4 is a summary showing the percentage of ^{1}H NMR spectra following Gaussian (rigid) and Lorentzian (fluid) distributions at T_{mf}, and T_2 values at this temperature. It also shows the η^*_{min} for comparison. T_{mf} is defined as the temperature of minimum η^* for rheometer measurements and the temperature of maximum percentage of fluid phase for ^{1}H NMR measurements.

Figures 9 and 10 show the percentage fluid phase and ^{1}H mobility of the fluid phase as a function of carbonization temperature for coal samples with particle sizes in the range of 53−212 μm. Table 5 shows a summary

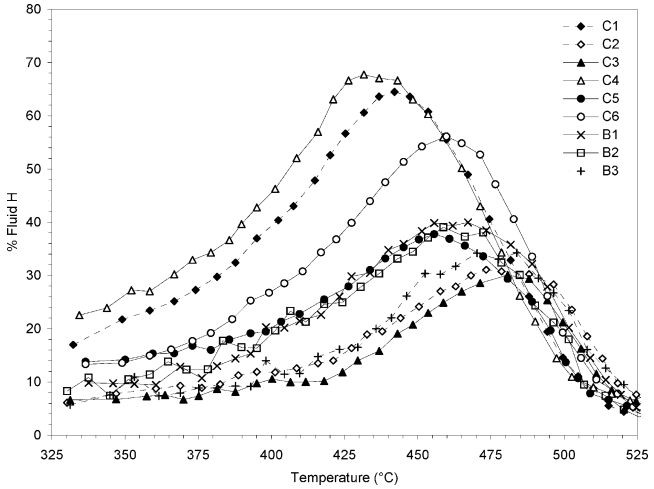

Figure 7. Percentage of the fluid phase as a function of temperature (particle size < 53 μm).

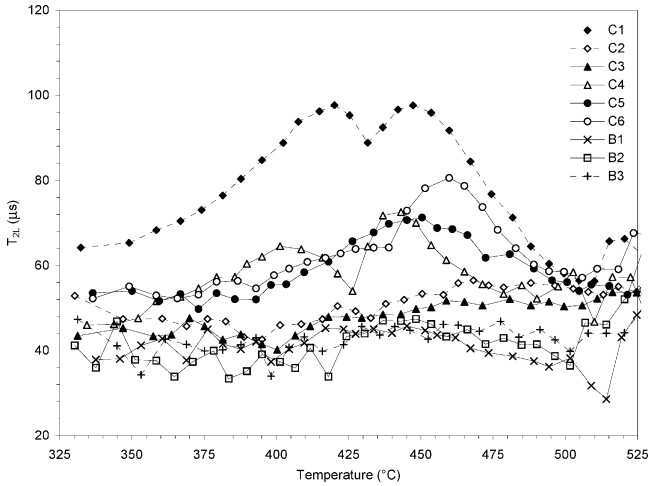

Figure 8. T_2 of Lorentzian distribution (T_{2L}) as a function of temperature (particle size < 53 μm).

Table 4. Temperatures of Maximum Fluidity (T_{mf}) from Rheometer (R) and ^{1}H NMR Spectrometer (S), η^*_{min}, Percentage of ^{1}H NMR Spectra (based on area) Following Gaussian (G) (rigid) and Lorentzian (L) (mobile) Distributions at T_{mf}, and T_2 Values of G and L Distributions at T_{mf} (particle size < 53 μm)

	T_{mf} (°C)			^{1}H NMR spectra (%)[b]		T_2 (μs)[c]	
	R	S	η^*_{min} (Pa s)[a]	G	L	G	L
C4	444	432	1.3×10^4	32	68	20	64
C1	446	442	2.9×10^4	36	64	20	97
C6	455	460	1.0×10^4	44	56	19	81
B1	467	467	1.9×10^5	60	40	16	41
B2	471	459	1.2×10^5	61	39	16	43
C5	450	456	1.0×10^5	62	38	17	69
B3	485	484	2.1×10^5	66	34	16	43
C2	465	473	1.1×10^5	69	31	16	55
C3		481		70	30	17	52

[a] Error < ±2% of value. [b] Error < ±1% on value. [c] Error < ±2 μs on value.

of the percentage fluid phase and ^{1}H mobility (T_2 values) at T_{mf} for the larger particle size range. The samples show increased percentage and mobility of fluid phase compared to the smaller particle size range (<53 μm).

Discussion

The rheometer and NMR results for C1, C2, and C3 coals compare well and also compare well with results

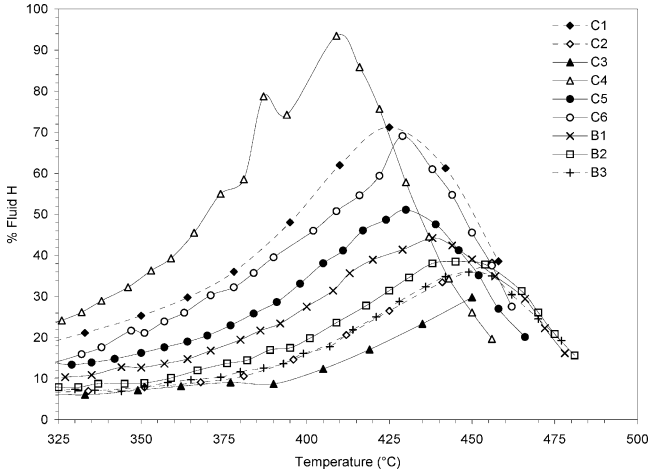

Figure 9. Percentage of the fluid phase as a function of temperature (particle size 53−212 μm).

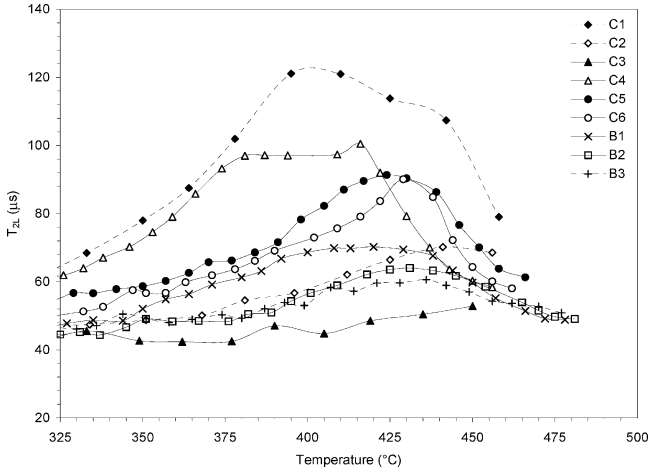

Figure 10. T_2 of Lorentzian distribution (T_{2L}) as a function of temperature (particle size 53−212 μm).

Table 5. Percentage of ^{1}H NMR Spectra (based on area) Following Gaussian (G) (rigid) and Lorentzian (L) (mobile) Distributions at T_{mf}, and T_2 Values of G and L Distributions at T_{mf} (particle size 53−212 μm)

	^{1}H NMR spectra (%)		T_2 (μs)	
	G	L	G	L
C4	7	93	13	97
C1	29	71	20	114
C6	31	69	25	90
C5	49	51	19	90
B1	56	44	18	68
B2	62	38	18	62
C2	62	38	16	69
B3	64	36	17	57
C3	68	32	18	58

obtained from the Gieseler plastometer. Both the temperatures at which changes occur and the magnitude of fluidity are fairly consistent. However, the Gieseler plastometer measured the same maximum fluidity of 37 ddpm for both C2 and C3 coals, which is not consistent with the rheometer and NMR results.

C1, C2, and C3 coals generated wall pressures of 3, 15.9, and 48.4 kPa, respectively. On the basis of the rheometer and NMR results, it appears that high wall pressures occur when only a small amount of fluid material forms and when this fluid material has a low mobility. It is thought that the coal particles fuse together and, due to the highly rigid nature of the mass,

volatiles are unable to permeate through and escape to the coal side where they build up in a diminishing region to a critical level, which causes the abrupt increase in pressure on the walls.

The rheometer, NMR, and Gieseler results also compare fairly well for B1, B2, and B3 blends. The temperature of maximum fluidity generally increases in the order B1 < B2 < B3, and both the percentage fluid phase and mobility of the fluid phase increase in the reverse order. The internal gas pressures measured during coking for these samples were 4.1, 5.8, and 12.9 kPa, respectively. The results assist the proposal made above that high gas pressures may occur when both the percentage of fluid material generated and the mobility of that material are low. In addition, it appears that the magnitude of pressure generated is directly related to T_{mf}—such that the higher the T_{mf}, the higher the gas pressure generated.

The rheometer, NMR, and Gieseler results for C4 coal compare well and are very similar to the results obtained for C1 coal. Both C4 and C1 coals formed large amounts of fluid material (>60%) which had high mobilities, and both generated low coking pressures of only 2 and 3 kPa, respectively. C5 also generated a low coking pressure of only 2.4 kPa, but the percentage of mobile ^{1}H was considerably less at approximately 38%. By comparison, the percentage of mobile ^{1}H for C2, which generated a significant coking pressure, was 31%. In addition, the ^{1}H mobilities in the fluid phase for these coals were 69 and 55 μs for C5 and C2 coals, respectively. It may be that there is a threshold for percentage and mobility of mobile ^{1}H, below which coking pressure is generated. This builds onto the mechanism proposed above. Perhaps when the percentage and mobility are both below approximately 40% and 65 μs, respectively, the pockets of fluid material do not link up to form passages of sufficient fluidity for gas to flow through the rigid network and out to the coke side. The gas is forced to the coal side, where it builds up. This threshold applies to particle sizes less than 53 μm. For particles in the size range 53−212 μm, the threshold is thought to be approximately 50% fluid phase with a mobility of 80 μs.

The reason the Gieseler and NMR measured a lower fluidity for C6 coal than C1 and C4 coals and yet the rheometer measured the highest fluidity for C6 coal is not known at this stage. C6 coal is known to generate significant and high wall pressures. The reason for this pressure is thought to be purely due to the coal charge expanding as it converts to gas and liquid phases. During some rheometer tests, the thickness of the sample was monitored. When only a minimal normal force was applied, C1, C4, and C6 coals expanded the most, with C6 expanding by almost 180% while C4 and C1 expanded by approximately 120%.

This work suggests that there may be two mutually exclusive mechanisms behind the generation of coking pressure, where the two extreme possible states for the fluid phase can lead to pressure on oven walls. This agrees with previous assessments, where the coking pressure curves suggest two mutually exclusive mechanisms.[2] Naturally, further tests on more coal samples need to be performed to confirm this hypothesis. The reason a model correlating Gieseler fluidity with coking pressure has not been established may be due to the problem coals being at either end of the fluidity spectrum. The Gieseler plastometer has been designed to be able to obtain empirical measurements of the fluid phase over a broad range of possible fluidities, but it may not cover the full range. The Gieseler gave similar fluidity values for C2 and C3 coals and yet these two coals behave very differently in the rheometer and NMR instruments and generate different coking pressures. At the other end of the range, the Gieseler recorded only 2954 ddpm for C6 coal yet this coal was found to be by far the most fluid coal measured using the rheometer. The main problem with the Gieseler plastometer is that it physically shears the sample and, considering that the fluid phase is shear thinning, this affects its properties. There is negligible movement of the sample in both the rheometer and NMR. Therefore, the rheometer and NMR maintain the physical properties of the samples better.

Conclusion

It is proposed that coking pressure may occur through two mutually exclusive mechanisms, with each case occurring when the fluidity is at either end of the fluidity spectrum. Coking pressure was found to occur for coals which formed only a small amount of fluid material (< ∼40%) and for which the ^{1}H mobility of the fluid phase was low (T_{2L} < ∼65 μs). The complex viscosity (η^*) of these samples did not decrease below 10^5 Pa s and the temperature of maximum fluidity (T_{mf}) was >465 °C. In this case it is proposed that the fused coal forms a rigid network containing pockets of fluid material which are largely unconnected and have a low fluidity. This network presents an impermeable barrier for gas flow, trapping the gas in the center of the coal charge where it builds up and eventually causes pressure to be exerted on the walls. The magnitude of the pressure generated for this mechanism may be inversely proportional to both the percentage and mobility of the fluid material, and proportional to the minimum η^* and T_{mf}. Coking pressure was also found to occur for a coal which formed a highly fluid phase over a broad temperature range. In this case it is proposed that the expansion of the coal charge as it converts to gas and liquid phases causes pressure to be exerted on the walls. The rheometer and NMR instruments used in this work have provided very precise characterizations of fluidity development at the microstructure level and could enable improved models to be developed for predicting coking pressure and coke quality.

Acknowledgment. The authors thank the European Coal and Steel Community for funding this work (Contract No.'s 7220-PR/069 and 7220-PR/119), the Instituto Nacional del Carbón in Spain and the Centre de Pyrolyse de Marienau in France for Gieseler and coking pressure data, and Rheometric Scientific for their technical assistance and helpful discussions.

EF034058L